

# fMRI Measurement of CMRO<sub>2</sub> Using a Comprehensive Biophysical Model: Compared with PET

A-L. Lin<sup>1</sup>, P. T. Fox<sup>1</sup>, J-H. Gao<sup>1</sup>

<sup>1</sup>Research Imaging Center, University of Texas Health Science Center at San Antonio, San Antonio, TX, United States

**Introduction:** Mapping changes in the cerebral metabolic rate of oxygen (CMRO<sub>2</sub>) in human brain during neuronal activation has been performed using both positron emission tomography (PET) and fMRI. It has been noted that the  $\Delta$  CMRO<sub>2</sub>/CMRO<sub>2</sub> measured by fMRI (based on a simplified biophysical model (1, 2)) in previous studies was significantly different both in its values and pattern of the frequency dependence when compared with those measured by PET. The simplified model is based on two approximations: (a) The relative cerebral blood volume (CBV), rather than being measured directly, was estimated based on a power-law relationship between CBV and blood flow (CBF); (b) The intravascular and extravascular components of BOLD signal, rather than evaluated separately, were mixed together. These approximations, if not valid, may cause problems in determining the relationships between CBF and CMRO<sub>2</sub>. Recently, a more comprehensive model which can eliminate the two approximations was proposed (3), and a novel fMRI data acquisition strategy was developed that enables us to measure changes in CBV (or VASO), CBF (or ASL) and BOLD simultaneously (4). We performed a visual fMRI study with five different visual stimulus frequencies with the novel sequence. The CMRO<sub>2</sub> changes as well as relationship between CBF and CMRO<sub>2</sub> was evaluated by both simplified and comprehensive fMRI models. The results from this fMRI study were further compared with those obtained from previous PET studies.

**Methods:** Experiments were performed on a 3T Siemens Trio MRI scanner. Eight healthy volunteers participated in this study. Visual stimulation was performed using a black-white checkerboard reversing its contrast at 1, 4, 8, 16, 32 Hz. The paradigm consisted of 3-min visual stimulus at each frequency alternating with 3-min baseline (eyes closed) condition. A single oblique axial slice (6 mm in thickness) encompassing the primary visual cortex was chosen for functional imaging. Pixel size was 4.1 × 4.1 mm<sup>2</sup>. EPI sequence was used with TR of 2 s and TE of 9.4, 11.6, and 28.1 ms for VASO, ASL, and BOLD images, respectively. Inversion slab thickness was 100 mm. TI<sub>1</sub> (blood nulling point) was determined empirically by searching for minimal signal intensity of the sagittal sinus area in the inversion recovery sequence (~680 ms), and TI<sub>2</sub> was 1200 ms. During an inversion recovery cycle, three images sensitive to VASO, ASL, and BOLD, respectively, were collected (4).

**Data Analysis:** The VASO image series was obtained by adding the adjacent slab-selective and nonselective images acquired from the first echo in the inversion recovery sequence. The ASL/BOLD image series was obtained by subtracting/adding the adjacent slab-selective and nonselective images from the second/ third echo in the sequence. Student's *t* tests were used to compare "baseline" and "stimulus" signals. Threshold was set to *t* = 3.0 (*P* < 0.005). Only the common activation pixels that passed the statistically significant threshold for all the VASO, ASL, and BOLD functional maps across all five visual stimulation frequencies were utilized for calculating average of the signal changes of the CBV, CBF, and BOLD, respectively.

## Model Comparison in calculating CMRO<sub>2</sub>:

### Simplified Model (2)

(a) Assuming a fixed relationship between CBV and CBF

$$\left(1 + \frac{\Delta CBV}{CBV_0}\right) = \left(1 + \frac{\Delta CBF}{CBF_0}\right)^a$$

in which '0' and 'Δ' are  $a=0.38$  (5) the change of the parameters, respectively.

(b) Did not separately evaluate intravascular and extravascular BOLD signals

$$\frac{\Delta BOLD}{BOLD} \equiv -TE \cdot \Delta R_2^*$$

assuming that change in transverse relaxation rate ( $\Delta R_{2i}^*$ ) is proportional to the concentration of deoxyhemoglobin [dHb], raised to an exponent  $\beta$  ( $1 < \beta < 2$ )

$$\Delta R_2^* = A \cdot [CBV \cdot [dHb]^\beta - CBV_0 \cdot [dHb]_0^\beta]$$

(c) Determination of CMRO<sub>2</sub> changes

$$\frac{\Delta CMRO_{2,0}}{CMRO_{2,0}} = \left(1 - \frac{(\frac{\Delta BOLD}{BOLD_0})^\beta}{M}\right)^{\frac{1}{\beta}} \cdot \left(1 + \frac{\Delta CBF}{CBF_0}\right)^{\frac{a}{\beta}} - 1$$

where  $M=0.24$  was determined by extrapolating from the value of  $M = 0.22$  at 1.5 T (2)

### Comprehensive Model (3)

(a) Direct measurement of CBV changes

$$\frac{\Delta CBV}{CBV_0} = -\left(\frac{C_{par}}{C_{blood} \cdot CBV_0} - 1\right) \cdot \frac{\Delta VASO}{VASO_0}$$

where  $C_{par}$  and  $C_{blood}$  are the water contents in ml water/ml substance for parenchyma and blood, respectively.

(b) Separate evaluation of intravascular and extravascular BOLD signals

$$BOLD \sim 0.3 \cdot x \cdot M_a e^{-R_{2a}^* TE} + 0.7 \cdot x \cdot M_v e^{-R_{2v}^* TE} + (1-x) \cdot M_t e^{-R_{2t}^* TE}$$

in which  $\chi$  is the water fraction of blood in the voxel,  $M_a$ ,  $M_v$ , and  $M_t$  are the magnetization of arteriole, venule and tissue, respectively, and  $R_{2i}^*$  ( $i = a, v, t$ ) is the effective relaxation.

(c) Determination of CMRO<sub>2</sub> changes

$$\frac{\Delta CMRO_2}{CMRO_{2,0}} = \left(1 + \frac{\Delta OEF}{OEF_0}\right) \cdot \left(1 + \frac{\Delta CBF}{CBF_0}\right) - 1$$

where  $OEF$  is oxygen extraction fraction.

### Coupling between CBF and CMRO<sub>2</sub> changes

$$n = \frac{\Delta\%CBF}{\Delta\%CMRO_2}$$

**Results and Discussion:** The changes in CBV, CBF and BOLD reached their maximum at 8 Hz (Figure 1). The change in CMRO<sub>2</sub> calculated with simplified model also reached its maximum at 8 Hz, while that calculated with comprehensive model reached a peak at 4 Hz and declined at higher frequencies (Figure 2). A statistically significant difference was found at all five frequencies between the changes in CMRO<sub>2</sub> determined by simplified and comprehensive models (*P* < 0.005) using Student's *t* test. Figure 3 shows that the coupling between changes in CBF and CMRO<sub>2</sub> obtained from simplified model is linear ( $n \sim 2.0$ ); whereas that obtained from comprehensive model is non-linear and is frequency dependent ( $n = 2.7-7.0$ ). As a consequence, a statistically significant difference existed at all five frequencies between the *n* values determined by the two models (*P* < 0.005). This observed discrepancy of the results between the two models is likely caused by the invalid assumptions used in simplified model. For example, the *a* value was fixed at 0.38 in simplified model, however, it was found that the *a* value can vary from 0.48-0.65 over the range of the five visual stimulus frequencies in this study. The experimental data shown in Figures 2 and 3 demonstrate that the CMRO<sub>2</sub> and *n* determined by the comprehensive model agree well with those obtained by previous PET studies (6, 7). In contrast, the results obtained from the simplified model show significant differences when compared with the PET measurements. By being able to eliminate the two assumptions, the comprehensive model has greatly enhanced the accuracy in the estimation of CMRO<sub>2</sub> and the *n* values.

**References:** (1) Hoge et al., *Proc Natl Acad Sci USA* 1999; 96:9403-9408. (2) Hoge et al., *Magn Reson Med* 1999; 42:849-863. (3) Lu et al., *J Cereb Blood Flow Metab* 2004 24:764-770. (4) Yang et al., *Magn Reson Med* 2004; 52:1407-1417. (5) Grubb et al., *Stroke* 1974; 5: 630-639 (6) Vafaei et al., *J Cereb Blood Flow Metab* 1999; 19: 272-277. (7) Vafaei and Gjedde, *J Cereb Blood Flow Metab* 2000; 20:747-754. \* Simplified Model; \*\* Comprehensive Model

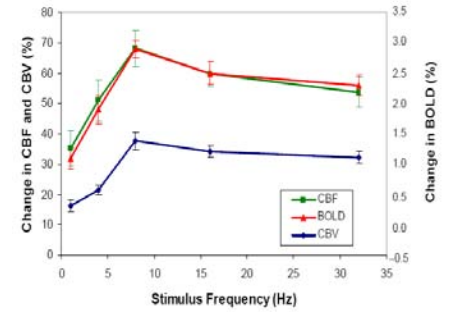


Fig. 1 Changes in CBF, BOLD and CBV at five stimulus frequencies

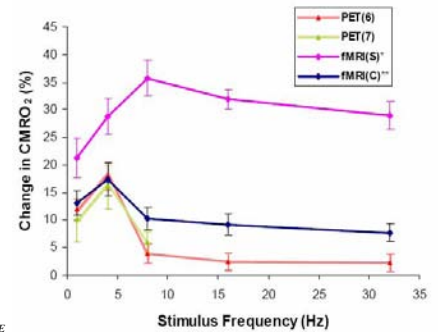


Fig. 2 Changes in CMRO<sub>2</sub> calculated by simplified and comprehensive models and their comparison to PET studies

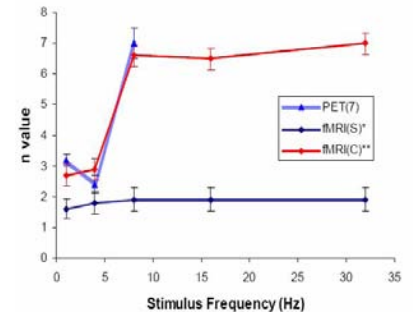


Fig. 3 Coupling ratio (*n*) of CBF changes to CMRO<sub>2</sub> changes obtained from simplified and comprehensive models and their comparison to PET study